Applied Catalysis B: Environmental 145 (2014) 108–119

Contents lists available at ScienceDirect

Applied Catalysis B: Environmental

journal homepage: www.elsevier.com/locate/apcatb

Synthesis and performance of highly dispersed Cu/SiO_2 catalysts for the hydrogenolysis of glycerol

E.S. Vasiliadou[b], T.M. Eggenhuisen[c], P. Munnik[c], P.E. de Jongh[c], K.P. de Jong[c], A.A. Lemonidou[a,b,*]

[a] Department of Chemical Engineering, Aristotle University of Thessaloniki, University Campus, GR-54124 Thessaloniki, Greece
[b] Chemical Process Engineering Research Institute (CERTH/CPERI), P.O. Box 60361 Thermi, Thessaloniki 57001, Greece
[c] Inorganic Chemistry and Catalysis, Debye Institute for Nanomaterials Science, Utrecht University, Universiteitsweg 99, 3584 CA Utrecht, The Netherlands

ARTICLE INFO

Article history:
Received 3 October 2012
Received in revised form
20 December 2012
Accepted 29 December 2012
Available online 9 January 2013

Keywords:
Glycerol hydrogenolysis
Cu/SiO_2 catalysts
Calcination treatment
Deactivation
SBA-15

ABSTRACT

The performance of Cu/SiO_2 (commercial silica gel, SBA-15 and SBA-15 treated at 900 °C) catalysts for the hydrogenolysis of glycerol to propylene glycol is investigated with emphasis on the stability characteristics. Cu catalysts with large crystals, small monodisperse crystallites or a highly dispersed XRD amorphous copper phase were obtained after calcination in stagnant air, in a flow of NO/N_2 or a flow of air, respectively. Analysis by XRD, N_2O surface oxidation and TEM confirmed the variation of the Cu specific surface area by the calcination conditions and the type of silica support used. The different dispersion characteristics resulted in different activities (20–50% glycerol conversion), while all the catalysts proved to be highly selective towards propylene glycol (92–97%). Present results indicate that glycerol hydrogenolysis over Cu-based catalysts is a structure sensitive reaction as significant variations in initial TOF were observed as a function of varying Cu crystallites. It is shown here that the presence of a solvent greatly influences the intrinsic reaction rate and the nature of structure sensitivity. The deactivation behaviour of all catalysts was studied, and based on detailed characterization of the spent samples it was attributed to Cu sintering and the presence of strongly adsorbed species on the catalytic surface. The 18 wt%Cu/silica gel (air) catalyst presented only moderate deactivation (~20%) while the catalyst supported on SBA-15 calcined at 900 °C (SBA900C) proved to be the most stable with negligible deactivation after three consecutive runs.

1. Introduction

The uncertain supply of fossil fuels and global warming problems result in an increase of renewable fuel production, especially of biodiesel from transesterification of vegetable oils and fats. The world production of biodiesel is estimated to reach 180 million tonnes by 2016, with an annual growth rate of almost 42% [1]. The overproduction of crude glycerol is a direct result of the increase in biodiesel production, as it is the by-product of the process. The latter created volatile pricing throughout the industry, while the demand for glycerol in general has remained stable. At present, the higher cost of biodiesel compared with petroleum diesel restricts its commercialization and usage. Alternative uses of glycerol are of great interest and will offer additional value to a biodiesel plant making the process economically feasible as well as overcoming the disposal problem of the surplus crude glycerol [2].

The transformation of glycerol to chemicals with added value that are currently produced from petroleum resources is considered as an attractive outlet. Hydrogenolysis of glycerol to 1,2-propanediol (propylene glycol) is one of the most promising routes to effectively utilize glycerol. This process provides an environmentally friendly and economically competitive route for the production of this important chemical compared with the currently used industrial method.

The selective hydrogenolysis reaction of glycerol to 1,2-propanediol takes place under hydrogen atmosphere in the presence of a suitable catalyst. The catalytic hydrogenolysis reaction has been extensively studied in various aspects, such as the development of effective catalysts [1,3–7], the improvement of reaction process [8–11] and more recently reaction kinetics [12,13]. Among the catalysts tested, mainly Ru [14–18] and Cu [3,6,8,19–23] exhibited high catalytic activity and selectivity towards 1,2-propanediol, with Cu showing superior performance in terms of selectivity. Other systems like Ni and Co have also been studied for this reaction [24–27]. The Ni-based catalysts tested present satisfactory activity, but the selectivity to the desired polyol is limited due to the formation of C—C bond breaking products (like ethylene glycol). The performance of the cobalt catalysts was

* Corresponding author at: Department of Chemical Engineering, Aristotle University of Thessaloniki, University Campus, GR-54124 Thessaloniki, Greece. Tel.: +30 2310 996273; fax: +30 2310 996184.
E-mail address: alemonidou@cheng.auth.gr (A.A. Lemonidou).

0926-3373/$ – see front matter © 2013 Elsevier B.V. All rights reserved.
http://dx.doi.org/10.1016/j.apcatb.2012.12.044

not so promising again in terms of propylene glycol selectivity, as ethylene glycol and other gas products formed resulted in about 50% selectivity values. In our previous studies we demonstrated the effect of catalyst acidity on glycerol hydrogenolysis by using different supports and metal precursors [28] and the influence of reaction parameters on stability and reaction pathways over Ru-based catalysts [29]. Unfortunately, Ru metal favours the formation of unwanted products, like ethylene glycol and gas products as ethane and methane due to the promotion of C—C bond scission of glycerol.

Copper is well known for the lower ability to cleave the C—C bonds of a glycerol molecule, resulting in less undesired degradation products. Various Cu-based catalysts have been evaluated for the hydrogenolysis reaction exhibiting excellent performance. Despite the activity and high 1,2-propanediol selectivity, disadvantageous deactivation of copper catalysts during the course of the reaction has been reported [1,6,30,31]. The decrease of the active Cu surface area along with sintering of Cu particles of a Cu/ZnO catalyst prepared by an oxalate gel method resulted in a strong deactivation of nearly 78% when the catalyst was used for a second time [6]. A similar deactivation pattern was observed for Cu/Al_2O_3 catalyst when collected and used for second time, even after a second pre-reduction [31]. Recently, the modification of a Cu/ZnO catalyst prepared by co-precipitation with Ga_2O_3 showed to enhance the performance in terms of stability after four hydrogenolysis runs with a glycerol conversion of ~55% and a 1,2-propanediol selectivity of ~83% at 200 °C and 50 bar of hydrogen. The role of Ga_2O_3 is attributed to a stabilizing effect preventing the metal particles from sintering [32].

Recently, we have developed effective copper catalysts supported on hexagonal mesoporous silica (HMS) and commercial silica [33]. It was shown that the highly dispersed copper particles are essential for the hydrogenolysis reaction. However, strong deactivation was observed for the best performing catalyst (20 wt%Cu/HMS). The loss in activity was associated with a number of factors like, copper particle sintering (decrease of active Cu surface area), partial collapse of the mesoporous structure of the support and carbonaceous deposits formed during the reaction.

The effect of thermal treatment (calcination) in order to prepare monodisperse nanoparticles from transition metal nitrate precursors on silica supports by impregnation and drying has been reported [34–36]. Wolters et al. [35] showed that during nitrate decomposition in a flow of 1% NO/N_2, the NO facilitates N—O bond cleavage of the nitrate, moderates the decomposition rate, scavenges oxygen radicals, and hence leads to high dispersions. For copper specifically, high metal surface areas were obtained by calcination in high flow gas streams [36]. While a flow of 1% NO/N_2 led to the formation of ~8 nm CuO particles on a commercial silica gel support, the calcination in a flow of air formed a highly dispersed amorphous copper phase. The effect of the thermal treatments as mentioned above is attributed to different decomposition mechanisms of the metal precursor nitrate salt. Both calcination methods led to high specific copper surface areas of 80–90 $m^2\,g^{-1}$. It is also very interesting to notice that copper supported on mesoporous silicas has attracted much attention due to the ability of tuning the porous characteristics of the host matrix and thus preparing metal or metal oxide nanoparticles on both the external surface and the inside of the pores [37].

The scope of the present work is to study the performance and especially the deactivation behaviour of highly dispersed Cu-based catalytic materials for the glycerol hydrogenolysis reaction. It is worth to mention that the catalysts used in this work are prepared via the simple impregnation and drying method which is advantageous compared to other complex synthesis techniques that are often applied. By varying the calcination conditions, highly dispersed catalysts are prepared with monodisperse nanoparticles or a highly dispersed amorphous copper phase and their deactivation behaviour is compared to a bench-mark catalyst, prepared under conventional conditions. Furthermore, we compare the effect of the support on catalyst stability by using a silica-type catalyst carrier with more stable porous characteristics. Emphasis is on the re-usability of the catalysts and on the characterization before and after the reaction in order to shed light on the factors which are determinant for stable performance.

2. Experimental

2.1. Catalyst preparation

2.1.1. Support materials

SBA-15 ($V_p = 0.91\,cm^3\,g^{-1}$, $S_{BET} = 864\,m^2\,g^{-1}$, $d_p = 8.7$ nm) was synthesized according to the procedure described by Zhao et al. using P123 as template and TEOS as silica source [38]. A gel with a molar composition of 1 SiO_2: 0.0143 P123: 5.05 HCl: 144 H_2O was aged under stirring at 40 °C for 20 h, after which it was treated at 80 °C for 48 h under static conditions. The precipitated white product was filtered, washed, dried at 120 °C and subsequently calcined at 550 °C for 6 h (heating rate 1°/min). The support is denoted as SBA. A sieve fraction of 38–75 μm was calcined at 900 °C for 5 h to further condense the silica matrix. The resulting SBA-15 is denoted SBA900C ($V_p = 0.34\,cm^3\,g^{-1}$, $S_{BET} = 271\,m^2\,g^{-1}$, $d_p = 6.5$ nm). Concerning the OH surface groups, it is well known from literature that ordered mesoporous silica generally has a low silanol surface density [39]. For the specific SBA-15 sample the starting silanol concentration was 1.01 OH/nm^2 while after heat treatment at 900 °C virtually no silanol groups were left (<0.05 OH/nm^2) as also evidenced by the fact that the sample had become hydrophobic [40]. Silica gel Davicat 1404 ($V_p = 0.87\,cm^3\,g^{-1}$, $S_{BET} = 458\,m^2\,g^{-1}$, $d_p = 7.2$ nm) was used as received from Grace-Davidson, and is denoted as SG. The density of surface silanol groups for the silica gel was determined as 2.9 OH/nm^2 using thermogravimetric analysis [40].

2.1.2. Catalyst preparation

Prior to impregnation the supports were sieved to a fraction of 38–75 μm. Supports were dried under dynamic vacuum at 60 °C for 30 min and let cooled to room temperature. Catalysts were prepared using pore volume impregnation with a 4 M $Cu(NO_3)_2$ aqueous solution ($Cu(NO_3)_2{\cdot}3H_2O$, 99% Aldrich). The impregnated support was dried at room temperature over night under dynamic vacuum. Typically 1.5 g of precursor loaded support was calcined in a plug-flow reactor under a flow of 1 L min^{-1} air or 1% NO/N_2 or air by heating to 350 °C for 30 min (heating rate 2 °C min^{-1}). As a bench mark catalyst, $Cu(NO_3)_2$/silica gel was calcined under stagnant conditions in ambient air by heating to 350 °C for 30 min (heating rate 2 °C min^{-1}). Catalysts thus obtained have a Cu loading of 18 wt% (SG and SBA supports) or 8 wt% (SBA900C support). Catalysts are denoted by the support (SG, SBA or SBA900C) and the calcination atmosphere (stag, NO or air).

2.2. Catalyst characterization

N_2-Physisorption measurements were performed at −196 °C using a Micromeritics Tristar 3000. The samples were dried prior to the measurement under an N_2 flow at 250 °C for at least 12 h. The total pore volume was defined as the single point pore volume at a relative pressure of $p/p_0 = 0.95$. The pore size distribution of the ordered mesoporous silica supports was calculated from the adsorption branch of the isotherm by a NL-DFT method designed for cylindrical pores. The pore size distribution of the silica gel was calculated from the desorption branch by BJH analysis. The maximum of the pore size distribution was taken as the average pore diameter.

XRD patterns were recorded for all catalysts between 10 and 60°2θ with a Bruker-AXS D2 using Co Kα_{12} radiation (λ = 1.790 Å). The diffraction patterns were normalized to the intensity of the amorphous silica scattering band (20–30°2θ). The volume average crystallite sizes were calculated from XRD line broadening using the Debye–Scherrer equation.

The reduction characteristics of the catalysts were studied by temperature-programmed reduction (TPR). These experiments were performed in a gas flow system equipped with a quadrupole mass analyzer (OMNI^{StarTM}, PFEIFFER). Typically, the catalyst sample (50 mg) was placed in a U-shaped quartz reactor and pretreated in flowing He (30 cm^3 min^{-1}) for 0.5 h at 250 °C, followed by cooling at room temperature. After pretreatment, the temperature was raised from room temperature to 400 °C at a rate of 10 °C min^{-1} in a 10% H_2/He flow (30 cm^3 min^{-1}).

The active copper metal surface area and particle size were determined by the dissociative N_2O adsorption method using the same apparatus as for TPR. In a typical experiment, the catalyst sample (20–50 mg) was placed in a U-shaped quartz reactor and pretreated in flowing He (30 cm^3 min^{-1}) for 0.5 h at 250 °C, followed by cooling at room temperature. The catalyst pre-reduction was performed by increasing the temperature to 230 °C with a ramp of 10 °C min^{-1} in a 10% H_2/He flow (30 cm^3 min^{-1}) for 1 h. Then the sample was cooled to 70 ± 5 °C in He flow and sequentially exposed to a N_2O flow, 30 cm^3 min^{-1} for 2 h, in order to oxidize the Cu^o surface to Cu_2O by adsorptive decomposition of N_2O. Finally, after further decrease of the temperature to ambient conditions, TPR was carried out on the freshly oxidized Cu_2O surface in order to reduce the Cu_2O to metallic Cu. In this step the temperature was increased from room to 300 °C with 10 °C min^{-1} using 10% H_2/He flow (30 cm^3 min^{-1}). The active copper metal surface area and particle size of the spent catalysts (after 2nd or 3rd time of use) were also measured by following the above procedure. Before N_2O titration the spent catalysts were oxidized with 10%O_2/He at 500 °C for 1 h in order to remove any possible adsorbed carbonaceous deposits from the surface. The treatment temperature was chosen after a TPO experiment following the CO_2 mass signal with the mass analyser. A comparative experiment was also performed without any treatment and the copper metal surface area calculated was lower (~24% compared with the measurement after the O_2/He treatment) leading us to the conclusion that at some extent the active Cu particles were covered by adsorbed species. Copper surface area and particle size were calculated according to data adopted from Ref. [41].

For the TEM measurements, the silica gel supported catalysts were embedded in a two component epoxy resin (Epofix, EMS) and cured at 60 °C overnight. The embedded catalysts were cut into thin sections with a nominal thickness of 50 nm using a Diatone Ultra 35° diamond knife mounted on a Reichter-Jung Ultracut E microtome. The sections were then collected on a TEM grid. Transmission electron microscopy was performed on a Tecnai 12 microscope operated at 120 keV.

An SDT Q600 (TA Instrument) thermogravimetric analysis (TGA) instrument was employed for the characterization of the used catalytic samples. SDT Q600 works in conjunction with a controller and associated software to make up a thermal analysis system. A small quantity of the sample was placed in an aluminium sample cup and the temperature was raised from room temperature to 700 °C at a rate of 10 °C min^{-1} in synthetic air flow (100 cm^3 min^{-1}).

2.3. Catalytic testing

Glycerol hydrogenolysis was carried out in a 450 ml stainless-steel batch reactor (Parr Instruments) equipped with an electronic temperature controller, a mechanical stirrer and a tube for the sampling of the liquid phase. Reaction was typically conducted under the following conditions: 240 °C temperature, 8 MPa hydrogen pressure, 0.35 g catalyst weight, 120 ml alcoholic (n-butanol) solution of glycerol 40 (v/v%), 5 h reaction time and 1000 rpm stirring speed. The stability of the catalytic materials was explored in repeated hydrogenolysis runs in order to test their reusability. Before every repeated hydrogenolysis test, the catalytic material was pre-reduced at 300 °C for 2 h under a stream of H_2/N_2 following the same procedure as for the fresh catalysts. The reaction was performed as follows: reactor loading with glycerol solution and the appropriate amount of pre-reduced catalyst, N_2 flushing for 10 min at 0.2 MPa, H_2 flushing for 5 min at 0.5 MPa, H_2 pressure set at 0.5 MPa and increase of temperature to 240 °C, finally, H_2 pressure increase to 8 MPa. The time at which both temperature and H_2 pressure reached the desired conditions (240 °C and 8 MPa) was selected as the zero point of the reaction time. However, as the temperature decreased by ~10 °C when H_2 was added to the system representative samples are considered after 1 h time on stream where the system was equilibrated. Then the reaction was allowed to run under the above mentioned conditions during which liquid samples were periodically removed. After each sampling, the reactor was back filled with hydrogen to retain a constant pressure. At the end of the reaction the system was allowed to cool down to room temperature and the gas products were collected in a gasbag.

Liquid samples were analyzed by GC (Agilent 7890A, FID, DB-Wax 30 m × 0.53 mm × 1.0 μm). Acetonitrile was used as a solvent for the GC analysis. The multiple point internal standard method was used for the quantification of the results. The liquid products detected were: 1,2-propanediol (propylene glycol), 1,3-propanediol, ethylene glycol, hydroxyacetone (acetol), 1-propanol, 2-propanol and methanol. Gas analysis was performed in an Agilent GC (7890A, Molecular Sieve and Poraplot) equipped with thermal conductivity detector. The gaseous products composed mainly carbon dioxide.

The conversion and selectivity terms were calculated using the equations described in previous work [28]. The initial turnover frequency, TOF, in h^{-1} was calculated as moles of glycerol converted per mole of surface metallic copper atoms during the first 1 h of testing at 240 °C, while the "steady state" TOF was calculated taking into account glycerol converted moles between the 4th and 5th reaction hours. It should be noticed here that the "steady state" TOF was calculated only for the most stable catalysts where the Cu particle size does not significantly change. The carbon balance in all experiments was better than 100 ± 10%.

3. Results and discussion

3.1. Structural characterization of the as-prepared catalysts

The composition, calcination conditions together with surface area and porous characteristics of the catalysts and supports are tabulated in Table 1. The decrease in pore volume and surface area observed for the catalytic samples supported on silica gel, compared with bare support, are assigned mainly to copper impregnation. For the two catalysts supported on SBA, Cu/SBA(air) and Cu/SBA(NO), this decrease appears to be significantly higher. This can only partially be attributed to the presence of copper, and some pore blockage or partial destruction of the mesoporous structure cannot be excluded. As mentioned above, in order to improve the structural stability of the catalysts with mesoporous silica carrier structure (SBA), the support was calcined at high temperature (900 °C). The heat treatment at 900 °C is proposed as a method for reducing the microporosity and stabilizing the mesoporous structure by further condensation of the silica matrix. Indeed, for SBA900C, the microporous volume determined with

Table 1
Physicochemical catalyst characterization.

Catalyst/support	Cu loading, wt%	Calcination method	BET surface area, $m^2\ g^{-1}$	Pore volume, $cm^3\ g^{-1}$	Pore diameter, nm	Cu dispersion[a]		
						S_{Cu}, $m^2\ g^{-1}{}_{Cu}$	S_{Cu}, $m^2\ g^{-1}{}_{cat}$	d_{Cu}, nm
Silica-gel (SG)	–	–	442	0.87	7.7	–	–	–
Cu/SG(stag)	18	Stagnant air	322	0.65	7.6	29	5.2	23.2
Cu/SG(NO)	18	Flow of 1%NO/N_2	385	0.64	7.3	70.6	12.7	9.5
Cu/SG(air)	18	Flow of air	315	0.62	7.3	87	15.7	7.7
SBA-15 (SBA)	–	–	828	0.87	8.7	–	–	–
Cu/SBA(NO)	18	Flow of 1%NO/N_2	512	0.53	8.5	68	12.2	9.9
Cu/SBA(air)	18	Flow of air	444	0.52	8.3	90	16	7.5
SBA calcined at 900 °C (SBA900C)	–	–	272	0.34	6.6	–	–	–
Cu/SBA900C(NO)	8	Flow of 1%NO/N_2	241	0.29	6.6	35	2.8	19.2
Cu/SBA900C(air)	8	Flow of air	202	0.24	6.3	7	0.6	96.1

[a] Determined by N_2O titration.

the t-plot method was 0.0 $cm^3\ g^{-1}$ compared to 0.11 $cm^3\ g^{-1}$, for the parent SBA. In addition, the total pore volume decreased to 0.34 $cm^3\ g^{-1}$ compared to 0.87 $cm^3\ g^{-1}$ for the parent SBA.

The effect of calcination conditions on the dispersion of Cu over silica gel supports was reported recently by Munnik et al. [36]. Calcining under stagnant air conditions leads to the formation of large CuO crystallites, while calcining under a flow of air leads to a highly dispersed XRD amorphous copper phase. The NO calcination method leads to the formation of small monodisperse CuO crystallites. These three calcination methods were applied here in the synthesis of the Cu based catalysts. The XRD patterns of the catalysts after calcination confirm the different dispersions obtained by the different calcination conditions (Fig. 1). For the bench-mark catalyst, Cu/SG(stag), sharp diffraction lines indicate the presence of large CuO crystals. Broad CuO diffraction lines were observed for Cu/SG(NO), which correspond to the formation of monodisperse small crystallites as has been reported earlier [36]. After calcination in a flow of air, only weak features are observed at the diffraction angles for CuO, indicating the formation of a largely XRD amorphous copper phase. For both SBA and SBA900C supported catalysts, similar observations were made. After calcination in a flow of NO/N_2 broad CuO diffraction lines indicate the presence of small crystallites. For Cu/SBA(air) some large extraporous copper crystallites were formed, as inferred from the sharp, low-intensity CuO diffraction, while for Cu/SBA900C(air), a larger amount of extraporous crystals was formed. The observations from XRD were confirmed with TEM. Fig. 2 shows typical micrographs for the SBA900C supported catalysts after calcination in a flow of air or NO/N_2. For Cu/SBA900C(air) (Fig. 2A), only seemingly empty support particles were observed. Cu/SBA900C(NO) (Fig. 2B) showed

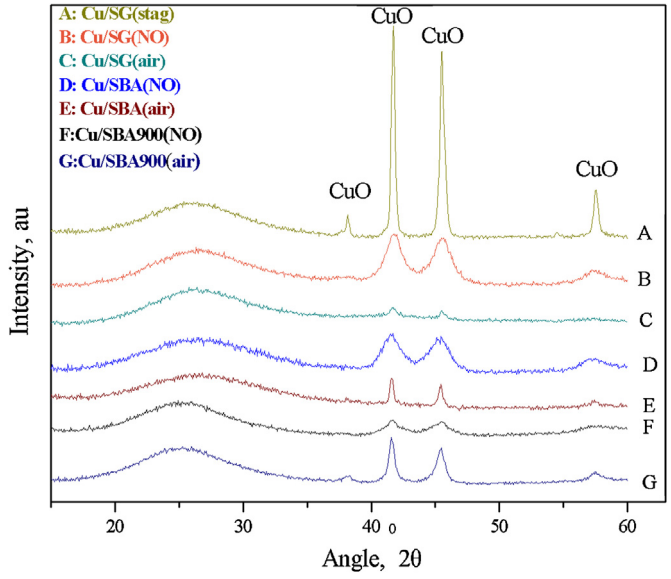

Fig. 1. XRD patterns of catalytic samples after calcination.

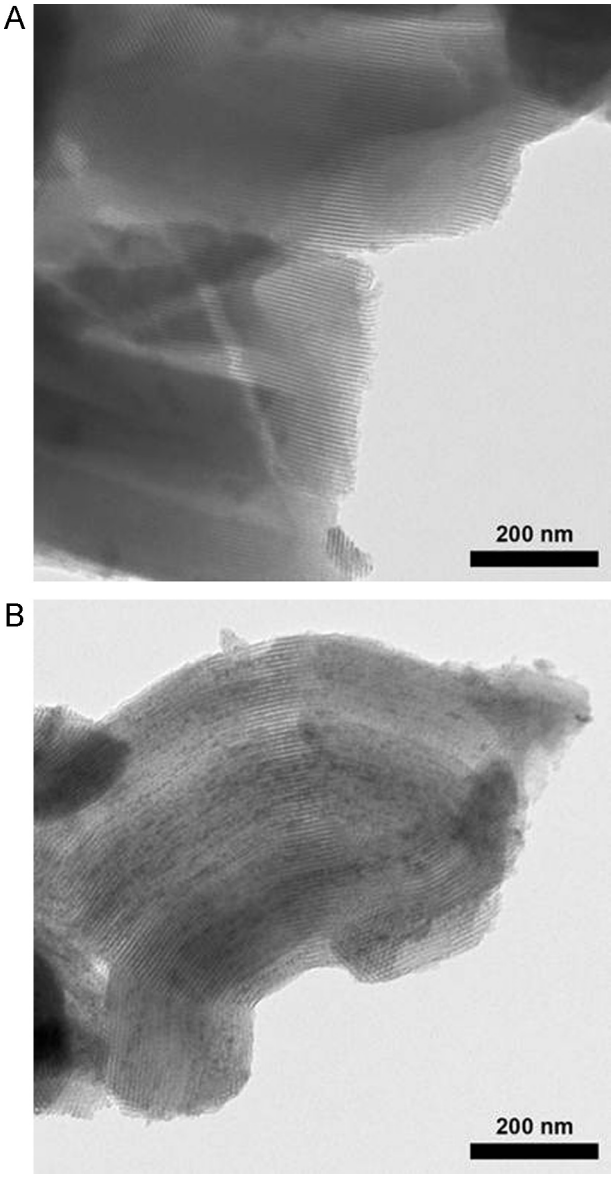

Fig. 2. TEM images of catalytic samples after calcination (A) Cu/SBA900C(air) and (B) Cu/SBA900C(NO).

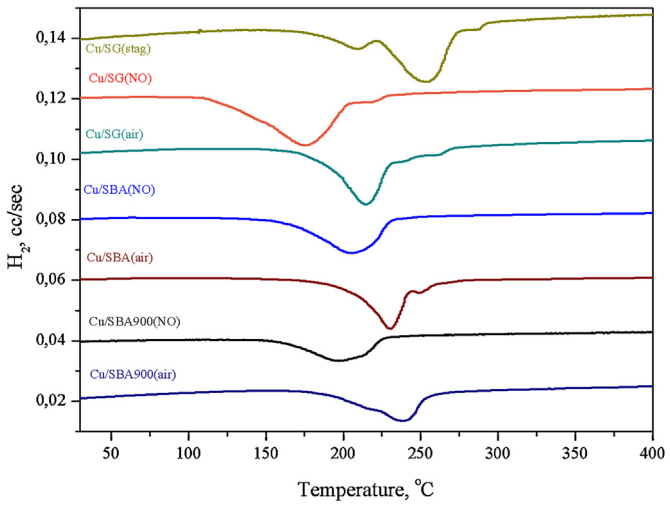

Fig. 3. TPR patterns of the catalysts.

pores filled with small copper particles after calcination, and a few larger particles on the exterior.

3.2. Characterization of activated catalysts

Temperature programmed reduction was employed to study the reducibility of the catalysts. Fig. 3 illustrates the hydrogen TPR profiles for all catalytic samples used in this study. The reducibility of the catalytic materials is also influenced by the calcination procedure (air/NO/stagnant air). In the case of air flow calcined samples there exists one main reduction peak and one or two small not well resolved shoulders located in the temperature region of 200–260 °C. These findings imply that the reduction of CuO to metallic Cu takes place via consecutive reduction steps [42]. The stagnant air calcined sample present almost the same reduction pattern with more intense shoulders. In addition, the reduction peaks are centred at broader temperature range of 180–280 °C. The shift of the reduction temperature to higher values reveals that this sample will be harder reducible compared with all the other catalytic materials treated under air or NO flows during calcination. The calcination with NO stream affects the reduction behaviour of the materials which exhibit one broad peak (except of the silica gel sample that also presents one small shoulder) instead of two or three as appear in the respective profile of the air flow calcined samples. In the case of the silica gel supported catalyst the peaks are located in a very broad temperature range of 110–225 °C, while in the case of the SBA supported catalysts the peaks are observed between 150 and 235 °C. It is also worthy to notice that the NO calcination treatment facilitates the reducibility, as in all cases the reduction temperature is lower. In addition, the symmetric profile of the reduction peaks evidences the homogeneity of the NO calcined catalysts and the formation of small monodisperse particles.

The active copper surface area and the corresponding copper crystallite size were measured with the dissociative N_2O adsorption method and the results are summarized in Table 1. The active copper surface area of the silica gel supported catalysts depends on the type of calcination treatment used. The bench-mark catalyst, Cu/SG(stag), has a copper specific surface area of 29 $m^2\ g_{Cu}^{-1}$. The calcination procedure under air flow positively affects the metallic copper surface area (87 $m^2\ g_{Cu}^{-1}$) corresponding to a Cu particle size of 7.7 nm. The use of NO during calcination resulted in a somewhat lower copper surface area (70.6 $m^2\ g_{Cu}^{-1}$) and a slightly larger particle size (9.5 nm). Similar surface areas were obtained for the SBA supported catalysts. For both SBA900C supported catalysts, a lower specific copper surface area was observed. It was also observed that in the case of the SBA900C support the use of NO compared to air flow favours the Cu surface area. This trend is firstly due to the lower surface area of the SBA900C support and secondly to its different porous characteristics compared with the silica gel and the SBA-15. Being more specific; the treatment at 900 °C further condenses the silica matrix, slightly decreases the mesopore diameter, but specifically removes almost all microporosity [43]. As a result probably the density of silanol groups that is needed as anchoring for the highly mobile anhydrous copper nitrate is too low, and hence larger crystals grow on the outside of the SBA particles.

The present results clearly show that the surface area of bare support and calcination procedure influence the copper species. It was observed that both supports possessing high surface area (Silica gel and SBA) lead to higher active metal areas (smaller metal particles) when air flow is used during catalyst calcination. For the SBA support with condensed matrix (after treatment at 900 °C) it was found that the calcination under a flow of air led to a very low active Cu surface area. These results were confirmed by observations from TEM and XRD. Fig. 4 shows typical micrographs for Cu/SBA900C after reduction. Some large copper particles were

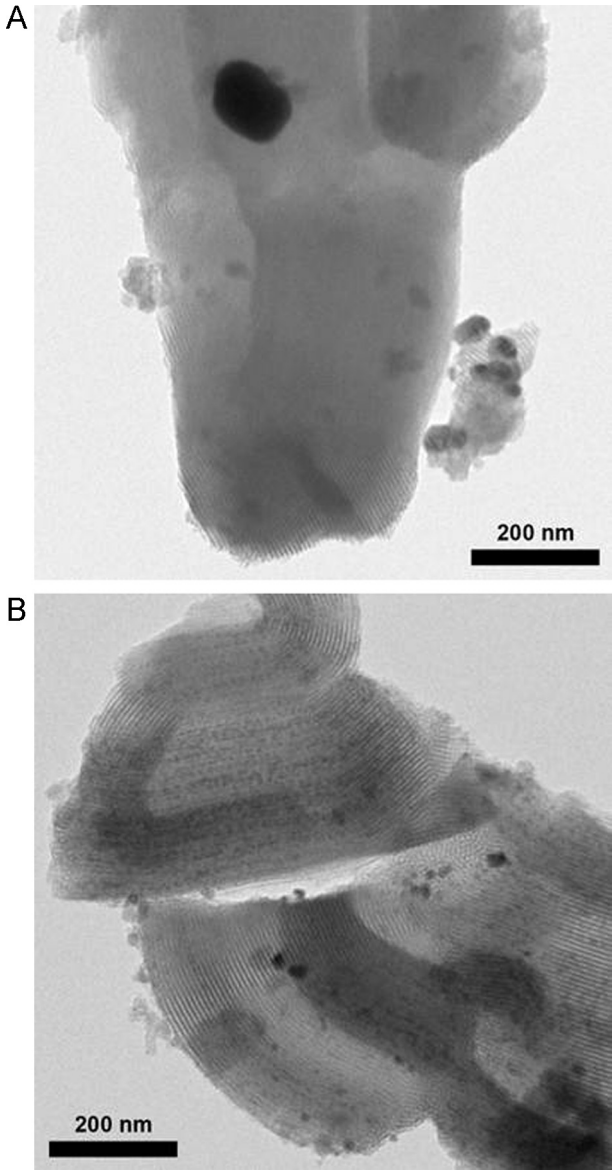

Fig. 4. TEM images of fresh catalytic samples after reduction (A) Cu/SBA900C(air) and (B) Cu/SBA900C(NO).

observed on the exterior of the support for Cu/SBA900C(air) and with XRD (not shown here) sharp diffraction lines for metallic Cu were observed. After reduction of Cu/SBA900C(NO), the pores of the support were filled with small copper particles, while some larger copper particles observed on the exterior of the support, while with XRD (not shown here) only broad Cu_2O diffraction features were observed. It seems that the reduction treatment also had an effect on Cu surface structure, as some large Cu particles were formed. This could be due to the migration and agglomeration of weakly interacting with the silica surface copper species [37].

3.3. Catalytic performance for the hydrogenolysis of glycerol

3.3.1. Product distribution as function of reaction time

The catalysts were tested at 240 °C and 8 MPa hydrogen pressure using an alcoholic solution of glycerol (40, v/v%) as the reactant for 5 h reaction time. Before testing, the catalysts were pre-reduced at 300 °C for 2 h under a stream of H_2/N_2. The temperature for the pre-reduction was selected based on the outcome of the TPR profiles. It was observed that with all catalysts the reduction of oxidic to metallic Cu form is completed at 300 °C.

In Fig. 5 the evolution of glycerol conversion and product selectivity as a function of reaction time is illustrated for two representative catalysts, Cu/SG(air) and Cu/SBA900C(air). In general, glycerol conversion gradually increased with reaction time and for Cu/SG(air) (Fig. 5A) reached a value close to 50% after 5 h. It should be underlined here that the conversion line does not start at the origin, as at reaction time zero and during the time needed for the reaction conditions to reach the values set and for the system to equilibrate, glycerol has been already converted to some extent (for details see Section 2). The main reaction product formed was 1,2-propanediol with selectivity values increasing from 91 to 97% over the reaction time, which was observed for the other catalysts as well. Somewhat different selectivity profiles of the products are observed for Cu/SBA900C(air) (Fig. 5B) which is also less active. The increment of 1,2-propanediol selectivity with time was more pronounced and coincided with a decrease of 1,3-propanediol and acetol selectivity during the reaction course. The selectivity for acetol, which is an intermediate product, decreases from ~6.5% to ~0.8% leading to an increase of 1,2-propanediol. The above result supports the dehydration/hydrogenation mechanism for the hydrogenolysis reaction [8,14,16,18]. As the route for 1,3-propanediol formation is parallel to that of 1,2-propanediol, the decrease in selectivity with the course of the reaction is ascribed to decreasing reaction rate for 1,3-propanediol formation. The selectivity of the degradation product (ethylene glycol) and over-hydrogenolysis products (propanols) remain unchanged at very low levels (ca. <2% and <1%) during the reaction over both catalysts. It is also worthy to notice that the only gas product formed is carbon dioxide with very low selectivity levels <0.5%.

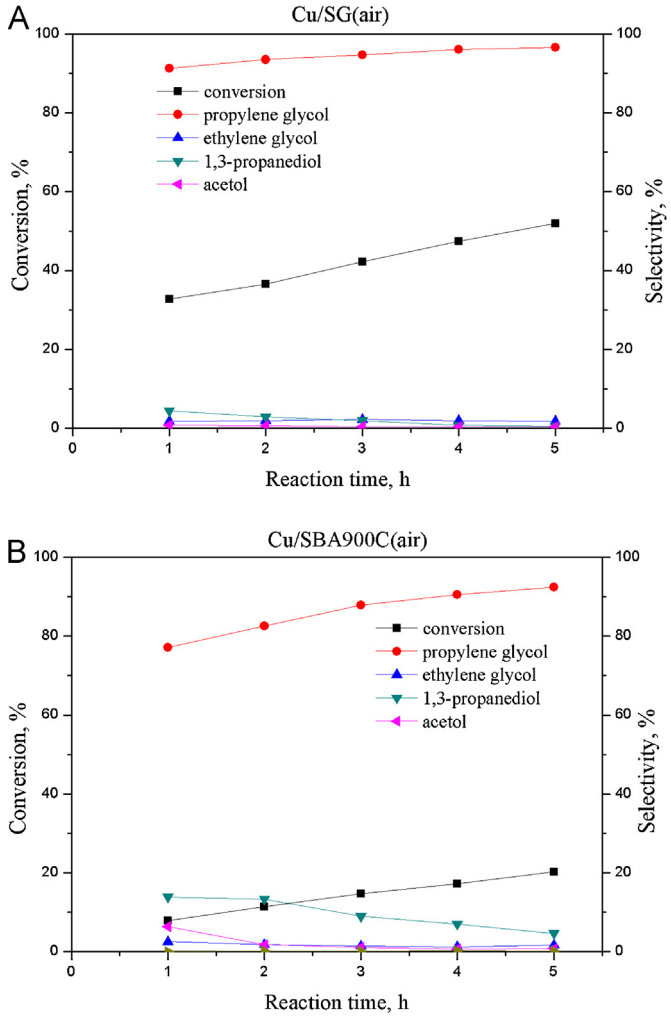

Fig. 5. Effect of reaction time on glycerol conversion and product distribution, temperature: 240 °C, hydrogen pressure: 8 MPa, weight ratio catalyst/glycerol: 0.006, reaction time: 5 h, (A) Cu/SG(air) and (B) Cu/SBA900C(air).

3.3.2. Evaluation of the catalysts on glycerol hydrogenolysis reaction

The activity, selectivity of the main products and TOF (h^{-1}) of all synthesized copper catalytic materials in glycerol hydrogenolysis reaction are summarized in Table 2. It is clear that the activity of the catalysts expressed as glycerol conversion depends greatly on the type of support and the calcination method used while the selectivity to propylene glycol remains unaffected at very high levels. Large variations in TOF values ranging from 260 to 620 h^{-1} are obtained among the catalysts. These values are extremely high compared to literature data pointing to the high activity of copper active sites of the catalysts under study. For example, the Cu:Al nano catalyst [44] at very similar reaction conditions, 220 °C and 7 MPa H_2 pressure, presents a TOF_{GLY} (h^{-1}) value of 10.2, which is more than an order of magnitude lower compared with the Cu/SiO_2 catalysts studied in the present work.

The results obtained for the silica gel supported catalysts reveal the important effect of the calcination procedure on the catalytic performance. The glycerol conversion of the catalysts calcined under flow conditions with air or NO/N_2 is higher (~50% glycerol conversion) compared with the bench-mark catalyst calcined under stagnant air conditions (~33% glycerol conversion). This result is associated with the higher active copper metal area obtained by optimizing the thermal treatment conditions during catalyst preparation. As measured by the N_2O surface oxidation method (Table 1) the samples calcined under flow conditions (air or NO/N_2) present high active Cu area, while the bench mark catalyst Cu/SG(stag) has lower active area.

For the SBA and SBA900C supported catalysts the different calcination atmosphere (air or NO flow) also influenced the catalytic activity. In the case of high loading samples (18%Cu on SBA) glycerol conversion presents only small differences concerning the effect of thermal treatment (compare 52.0 with 48.8%). The effect of different calcination atmosphere is more pronounced with the SBA900C supported catalysts. The NO calcined sample results in higher glycerol conversion compared with the air treated one. This behaviour can be explained using data from N_2O surface oxidation, XRD and TEM characterization. The air-calcined sample after reduction presented almost empty pores with large copper particles on the exterior of the support. On the other hand, the NO

Table 2
Catalytic results of glycerol hydrogenolysis over Cu/SiO_2 catalysts (reaction conditions: 8 MPa hydrogen pressure, 240 °C, weight ratio catalyst/glycerol: 0.006, 5 h).

Catalyst	Conversion, %	Selectivity, %			Initial TOF, h^{-1} [a]
		Propylene glycol	Ethylene glycol	Propanols (1- and 2-)	
Cu/SG(stag)	32.7	94.3	1.3	0.09	499
Cu/SG(NO)	50.7	95.4	1.8	0.6	293
Cu/SG(air)	51.9	96.6	1.8	0.09	263
Cu/SBA(NO)	48.8	95.9	1.9	0.2	342
Cu/SBA(air)	52.0	96.2	1.8	0.1	283
Cu/SBA900C(NO)	37.4	95.6	1.4	–	450
Cu/SBA900C(air)	20.3	92.4	1.7	0.2	621

[a] Initial TOF was calculated based on data collected after 1 h reaction time.

calcined catalyst showed pores filled with small particles, with a few larger particles on the exterior leading to higher active copper metal area and hence to higher activity.

Concerning the desired product selectivity, the values obtained for almost all tested catalytic materials are very high (92–97%) confirming the superior performance of Cu-based catalysts. The efficiency of copper for C—O hydro/dehydrogenation is well established in literature [45], but it is also worth mentioning that in the presence of these catalytic materials the extent of excessive hydrogenolysis of propylene glycol to propanols is negligible (selectivity values lower than 0.25%) compared with Cu—Cr catalyst [4]. The latter catalyst prepared by a sol gel non-alkoxide route resulted at high 1-propanol (36%) selectivity lowering the selectivity of propylene glycol to 54%. In the presence of Cu/SiO_2 catalysts used in this study the productivity of propylene glycol ranges from 5.5 to 15 $g_{1,2\text{-PDO}}\ g_{cat}^{-1}\ h^{-1}$, values which are several times higher than that of other catalytic systems. Although, a direct comparison is not possible due to the different operating conditions used from different research groups it is worth to mention some previous studies. For example, a CuO/ZnO catalyst prepared by an oxalate gel co-precipitation method results in 1.5 $g_{1,2\text{-PDO}}\ g_{cat}^{-1}\ h^{-1}$ at 200 °C, 5 MPa H_2 after 7 h reaction time [6] while, the Cu:Al catalyst prepared by co-precipitation leads to the production of 3.3 $g_{1,2\text{-PDO}}\ g_{cat}^{-1}\ h^{-1}$ at 240 °C, 7 MPa H_2 after 5 h [44].

The activity, expressed as the reaction mass specific rate (moles glycerol converted $h^{-1}\ g_{cat}^{-1}$) is clearly correlated with the active copper surface area (S_{Cu}, $m^2\ g_{cat}^{-1}$) as shown in Fig. 6. This correlation exists for the initial as well as for the rate after 5 h reaction time. The increase the mass specific rate with increasing S_{Cu} demonstrates the decisive role of initial copper surface area in hydrogenolysis reaction. Some observed deviations from linearity may be due to surface oxidation part of the metallic Cu to Cu_2O during the reaction course, as has been reported also for methanol synthesis over a Cu catalyst [46]. The figure also shows that even in the absence of an active catalyst, glycerol can be converted thermochemically at some extent, as the line does not go through the origin.

An attempt to correlate the initial intrinsic activity, expressed as turnover frequency per hour (Table 2) with Cu average particle size as measured by dissociative N_2O adsorption method (Table 1) is presented in Fig. 7. The 1 h time-on-stream experimental data were used for the calculation of TOF in order to minimize possible effect from deactivation phenomena. As seen in Fig. 7, the initial rate per active Cu site depends strongly on the metal particle size, demonstrating thus the structure sensitivity of the glycerol hydrogenolysis reaction. The initial intrinsic rate per active site increases as Cu particle size increase. Geometric factors can explain the differences in the intrinsic activity of small particles below 10 nm. However, effects for particle sizes from 10 to 100 nm are not straightforward related with the geometric configuration, but can be understood taking into account changes in the electronic properties of the metal particles. Vannice and coworkers [47] observed the same trend in acetone hydrogenation over copper on silica catalysts with varying particle size up to 110 nm. They ascribed this to differences in the adsorption behaviour of reactants and/or products which consequently affect the reaction rates. Fig. 7 also presents the "steady state" TOF for the two most stable (see below Section 3.3.3) catalysts. These two materials were selected here to show the particle size effect during the reaction course. Larger copper particles (8Cu/SBA900C(air)) present higher turnover rates compared

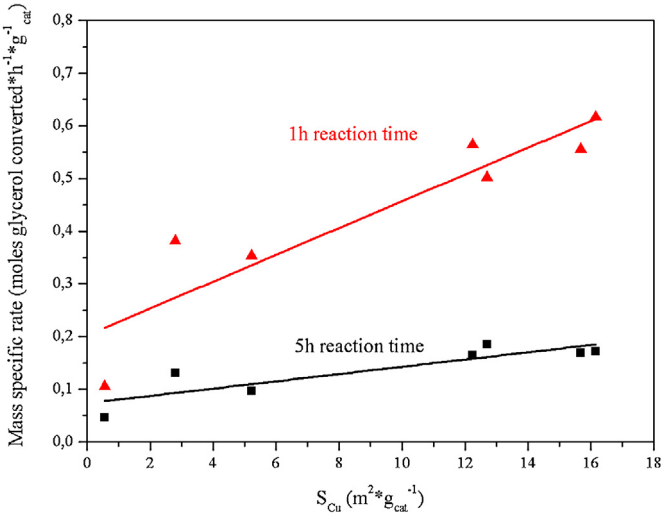

Fig. 6. Mass specific rate as a function of copper surface area for fresh catalysts (conditions: temperature: 240 °C, hydrogen pressure: 8 MPa, weight ratio catalyst/glycerol: 0.006, reaction time: 1 and 5 h).

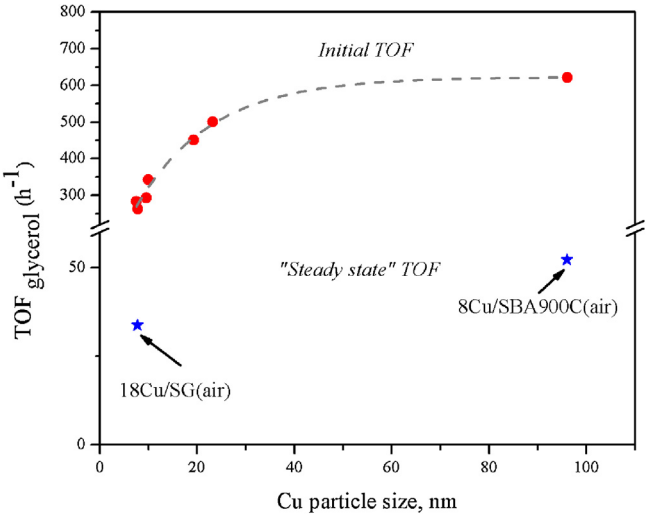

Fig. 7. Initial and "steady state" turnover frequency of glycerol as a function of copper particle size (conditions: temperature: 240 °C, hydrogen pressure: 8 MPa, weight ratio catalyst/glycerol: 0.006).

with smaller ones (18Cu/SG(air)) and thus the same trend as for initial values is observed, although less pronounced (45% vs 100%). It is clearly shown from Fig. 7 that the initial turnover frequency after 1 h is remarkably higher compared with "steady state" TOF after 5 h reaction time.

The observation of structure sensitivity is in line with our previous findings about the size-dependency of this reaction over Cu on silica catalysts [33]. However, in the present study it was found that the type of structure sensitivity changes, as TOF increases with Cu particle size increment. In addition, higher values of TOF were obtained with the present catalysts. Worthy to note that the evaluation tests in the present study were performed employing an alcoholic solution and not pure glycerol as that of the previous study. To explore the role of the solvent on intrinsic activity, experiments with two catalytic samples, Cu/SG(NO) and Cu/SG(air), using pure glycerol and alcoholic glycerol solution were conducted. The results obtained clearly revealed the significant effect of the solvent on the TOF which increased by almost 20% when the solvent was present. The positive effect observed can be attributed to increased H_2 solubility in the liquid phase in the presence of the solvent and stabilization of reactive intermediates formed. Zhang et al. [48] studied the methanol synthesis using Monte Carlo simulation and found that the intrinsic rate depended not only on the number of activity sites, but also on the ratio of different adsorbed species on the catalyst surface. Therefore it was postulated that increased hydrogen solubility is associated with optimized ratio between the adsorbed species favouring thus the intrinsic rate. The observation of structure sensitivity alteration although not expected based on our previous findings, has been reported by other research groups as well [49,50]. The group of Prof. Jackson [49] observed different structural sensitivity for nitrobenzene hydrogenation reaction in the liquid phase over Pd/C catalysts depending on the solvent used. The change in structural sensitivity is explained by considering that the properties or the environment generated by the solvent are associated with a change of the rate determining step. A change in the reaction mechanism such as this, could explain the differences on turnover rate induced by the presence of a solvent in the reaction mixture.

3.3.3. Catalytic stability

According to the literature, copper catalysts in glycerol hydrogenolysis reaction suffer from serious deactivation problems [1,6,30,31]. The deactivation behaviour was attributed mainly to the loss of active surface area. The activity loss of these copper catalysts during reaction constitutes the main obstacle for their industrial application. In our previous study, we reported that the excellent performance of copper based on mesoporous hexagonal silica support in terms of activity (turnover frequency) and 1,2-propanediol selectivity in the first usage is not observed after the second usage time [33]. The improvement of catalyst stability is tackled herein by employing various silica-type supports with different porous characteristics and thermal treatments, as above presented. The stability was tested for all the catalytic samples in a second run and the most stable materials were used for a third reaction run. The collected catalysts were washed and dried at 120 °C overnight and reduced under hydrogen flow at 300 °C before further testing. Table 3 summarizes glycerol conversion and 1,2-propanediol selectivity with usage times.

Comparing the deactivation behaviour of the catalysts (Table 3), the activity loss follows the order Cu/SG(NO) > Cu/SBA(NO) > Cu/SG(stag) > Cu/SBA900C(NO) > Cu/SBA(air) > Cu/SG(air) > Cu/SBA900C(air) after the second usage time. The two more stable catalysts Cu/SG(air) and Cu/SBA900C(air), were used for a third time. In the case of the silica gel supported catalyst Cu/SG(air), the activity was moderately decreased compared with the second hydrogenolysis run. On the other hand, the Cu/SBA900C(air) catalyst exhibited stable behaviour during the three catalytic cycles used. The loss in conversion was negligible as shown from Table 3 (0.9% loss). As a general trend the NO and stagnant air calcined samples, present lower resistance to deactivation compared with the air flow treated catalysts. Concerning 1,2-propanediol selectivity, the results were only slightly affected by usage times, for all catalysts independently of their deactivation behaviour.

The surface oxidation with N_2O technique was applied for spent catalysts to measure the active surface area of copper and the results are also compiled in Table 3. Before measuring, each sample was oxidized with 10% O_2/He at 500 °C for 1 h in order to remove any possible adsorbed surface species and carbon deposits. Decrease of the active surface Cu was observed for all the spent catalysts except for the Cu/SBA900C(air) sample. These results nicely correlate with the deactivation degree of the catalysts. The Cu/SBA900C(air) catalyst showed excellent stability after three times reuse and no loss in Cu active area. Although the numbers (% decrease of active surface area) do not match exactly with the deactivation degree for each catalyst, it is proposed that the loss of active metal area is the main factor for catalyst deactivation. Correlating the Cu surface area (S_{Cu}, $m^2\ g_{cat}^{-1}$) of the used catalysts (Table 3) with the mass specific rate after 5 h for the respective reusage time it is obvious that the two parameters are linearly correlated (Fig. 8). Cu/SG(NO) showed deviating behaviour, as the activity of this catalyst is much lower than what would be expected based on the Cu surface area (see data point indicated by arrow in Fig. 8). This result implies that other factors than copper agglomeration, also contribute to the observed deactivation.

Focusing on the silica gel supported catalysts it was shown that the performance of both samples (air and NO) in the first time use does not present any significant differences, as both result in almost the same glycerol conversion (~50%) along with 1,2-propanediol selectivity (~96%). However, the NO calcined catalyst presents a tremendous decrease on its activity (59.4%) after the second experimental run and also a slight decrease in the selectivity of the desired product (from 95.4 to 89.1%). On the contrary, the silica gel air-calcined sample showed resistance to deactivation after three times of use in the hydrogenolysis reaction (deactivation degree 21.6%). The activity of this catalyst ranged from 52 to 41%, while 1,2-propanediol selectivity remained constant at an average value of ~96%. The catalyst Cu/SG(stag) presents a lower degree of deactivation (40.7%) compared with Cu/SG(NO) after the second cycle

Table 3
Reusability results of glycerol hydrogenolysis over Cu/SiO_2 catalysts (reaction conditions: 8 MPa hydrogen pressure, 240 °C, weight ratio catalyst/glycerol: 0.006, 5 h).

Catalyst	Conversion, % (1st time)	Conversion, % (2nd time)	Conversion, % (3rd time)	Deactivation degree, %	S_{Cu}, $m^2\ g_{Cu}^{-1}$ (used)	S_{Cu}, % decrease
Cu/SG(stag)	32.7	19.4	–	40.7	17.6	39.3
Cu/SG(NO)	50.7	20.6	–	59.4	35.2	50.1
Cu/SG(air)	51.9	47.7	40.7	21.6	49.4	43.3
Cu/SBA(NO)	48.8	28.4	–	41.8	24.8	63.5
Cu/SBA(air)	52	40.2	–	22.7	36.4	59.4
Cu/SBA900C (NO)	37.4	25.7	–	31.3	15.5	55.7
Cu/SBA900C (air)	20.3	17.4	20.1	0.9	9.8	0.0

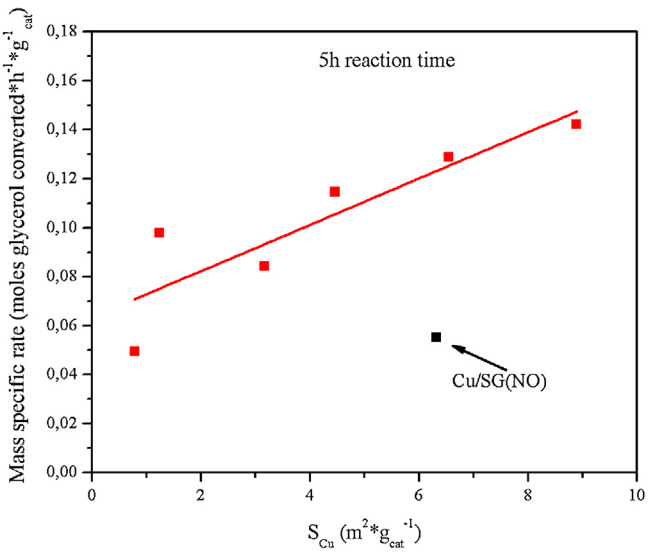

Fig. 8. Mass specific rate as a function of copper surface area for used catalysts (conditions: temperature: 240 °C, hydrogen pressure: 8 MPa, weight ratio catalyst/glycerol: 0.006, reaction time: 5 h).

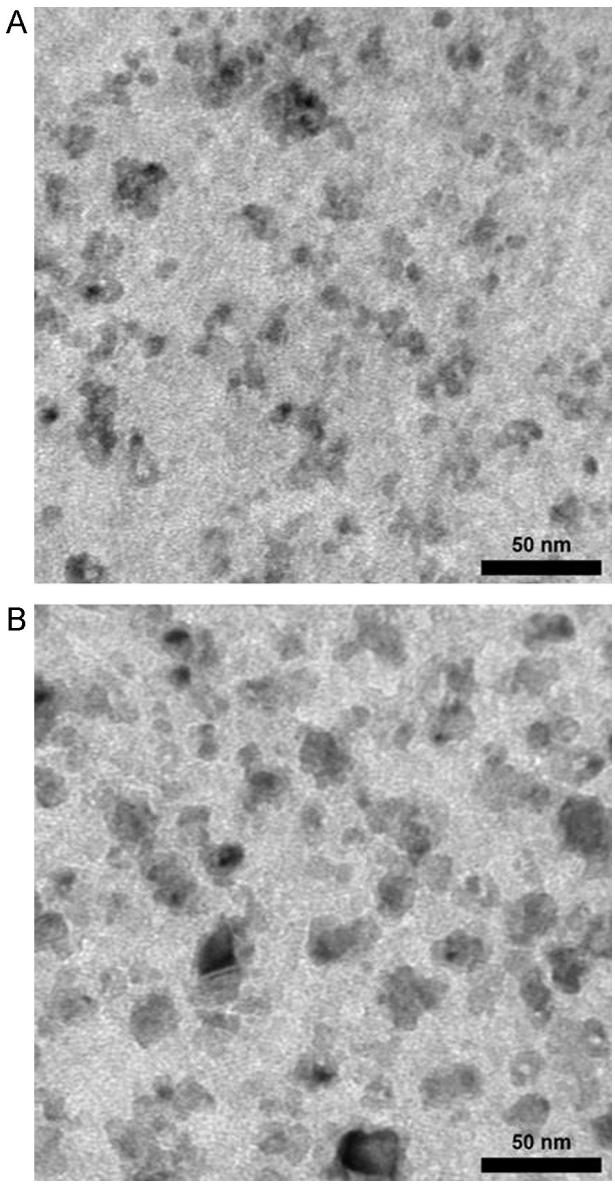

Fig. 9. TEM ultramicrotomy images of (A) 3rd time used Cu/SG(air) and (B) 1st time used Cu/SG(NO) catalysts.

of reaction, with a small decrease in selectivity of propylene glycol (from 94.3 to 89.4%).

As mentioned above, our intention was to stabilize the SBA structure through the thermal treatment of the parent SBA at high temperature (900 °C). Comparing the degree of deactivation of the respective samples, Cu/SBA(air)–Cu/SBA900C(air) and Cu/SBA(NO)–Cu/SBA900C(NO) it seems that the goal has been achieved. For samples prepared under same calcination atmosphere (NO or air) the deactivation degree of those supported on SBA900C is much lower (Table 3). Furthermore, the Cu/SBA900C(air) catalyst showed no deactivation during the three cycles of reaction. One might argue that the low activity of this sample (20% conversion) is the reason for the good stability. However, paying attention to the results presented in Table 3, it is clear that other samples with low activity like the Cu/SG(stag) are not stable presenting loss of activity in the range of 40%. Therefore, the high stability of the Cu/SBA900C(air) catalyst is tentatively ascribed to the morphology characteristics of the support and the calcination treatment which increase the resistance to harsh conditions (high pressure, liquid phase).

3.4. Structural characterization of spent catalysts

All the catalysts used for repeated hydrogenolysis cycles were characterized by various techniques and compared with the fresh calcined and reduced samples in order to shed light onto their performance and behaviour in terms of stability.

TEM of ultramicrotomed slices provided additional information on the morphology of the spent Cu/SG(air) and (NO) samples. As can be seen from Fig. 9, the difference in the size distribution of Cu particles of the samples is evident. The spent Cu/SG(air) catalyst showed particles with an average size of ~10 nm even after the third cycle very close to the size of the fresh sample (compare with Table 1). In contrast, the catalyst calcined in NO/N_2 (Cu/SG (NO)) displayed much larger particles between 10 and 30 nm, a distinct change compared with the fresh sample (d_{Cu} = 9.5 nm).

The spent catalysts supported on SBA and SBA900C were also characterized by TEM (Fig. 10). For the SBA supported spent catalysts, extensive migration of the active copper phase to the exterior of the support became apparent. Although some particles were still observed within the pore system, mainly large agglomerates were observed on the exterior of the support. A close look at the particles on Cu/SBA(air)-spent, showed that they are polycrystalline, which gives an explanation for the absence of sharp diffraction lines in the XRD pattern (not shown here). For Cu/SBA(NO)-spent, more particles were still observed within the pore system, but also many large particles were observed on the exterior of the support. Concerning the spent SBA900C supported catalysts the difference on the morphology between them is clearly shown. In agreement with the active copper surface of the spent catalyst, TEM image indicate a low degree of sintering for the sample Cu/SBA900(air). In contrast, large square shaped particles exist on the exterior of the support of the used catalyst Cu/SBA900C(NO).

As shown from the results of the stability tests and characterization by surface oxidation with N_2O and TEM, sintering of copper is the key factor for the observed loss in activity. The deactivation of the catalysts could be largely explained by the decreased specific copper surface area. Nevertheless, for example Cu/SG(NO), showed a larger degree of deactivation than expected from the loss of its active area (see Fig. 8). Therefore, further characterization of the used samples was attempted employing thermogravimetric

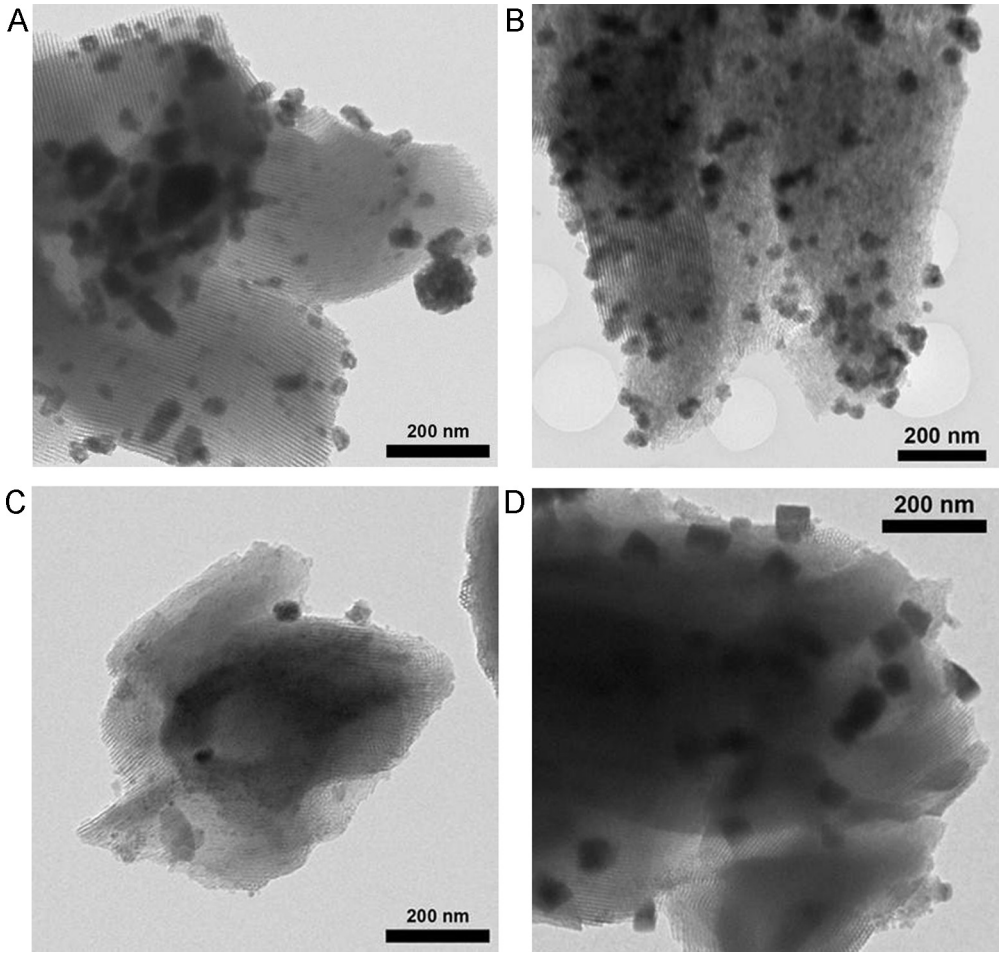

Fig. 10. TEM images of used catalysts (A) Cu/SBA(air), B) Cu/SBa(NO), (C) Cu/SBA900C(air) and (D) Cu/SBA900C(NO).

analysis to detect strongly adsorbed species and carbonaceous deposits. Fig. 11 shows the weight loss vs temperature for all the spent catalysts under oxidizing conditions. Wide variations were observed in the weight loss profiles of the different catalysts. The weight decrease up to 200 °C was assigned to water loss, while the weight loss between 200 and 300 °C is associated with the presence

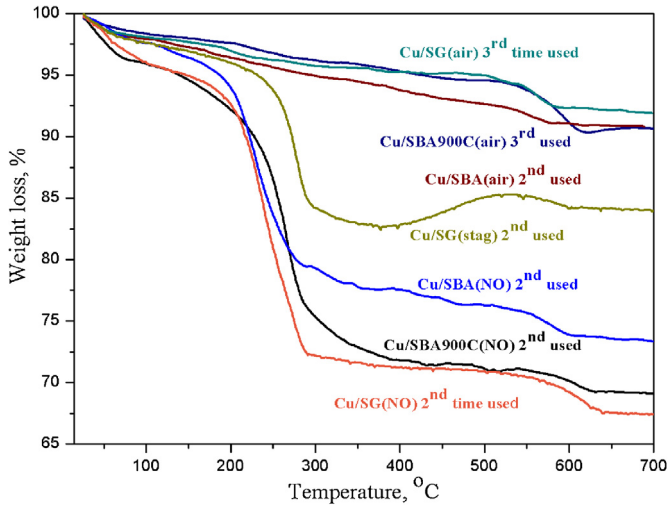

Fig. 11. Thermogravimetric analysis in oxidative atmosphere of the used catalysts in glycerol hydrogenolysis.

of strongly adsorbed components (reactant and/or products) on the catalyst surface. Finally, the weight change taking place at higher temperatures was attributed to the removal of carbonaceous deposits (coke). The largest weight loss was observed between 200 and 300 °C, due to the presence of adsorbed species that may also contribute to deactivation by blocking the active catalytic sites. This observation could explain the deviating behaviour of the Cu/SG(NO) catalyst discussed above. This catalyst shows drastic decrease in its weight, implying high degree of surface covered by adsorbed species. In addition, all the spent samples presented 3–6% weight loss at high temperatures due to carbonaceous deposits. The presence of these deposits contributes also to deactivation. The weight loss profile of the spent Cu/SG(stag) shows weight increase at maximum temperature ~520 °C due to oxidation of metallic copper to copper oxide. The latter was not observed for the other spent catalysts probably due to compensation of the phenomena of oxidation and removal of surface carbon species. It is worth to notice that the stable behaviour of the catalysts Cu/SG(air) and Cu/SBA900C(air) is also characterized by low weight loss during thermogravimetric analysis.

The structural integrity of the spent catalysts was analyzed by N_2-physisorption. The isotherms of the SG support and Cu/SG(air) fresh and spent catalyst are shown in Fig. 12. After reaction, the total pore volume did not decrease significantly compared to the calcined system. However, the hysteresis shifted to higher relative pressures, indicating widening of the pore system. The stability of the SBA and the thermally treated SBA900C supports under reaction conditions, were also studied and the isotherms are shown

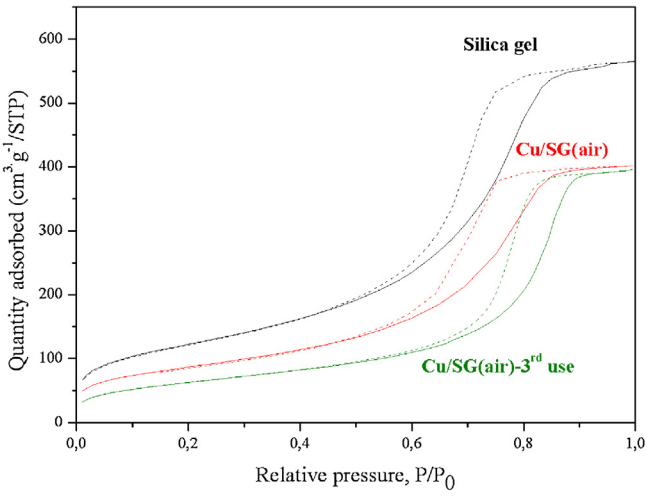

Fig. 12. N_2-physisorption curves of silica gel, Cu/SG(air) as prepared and Cu/SG(air) 3rd time used.

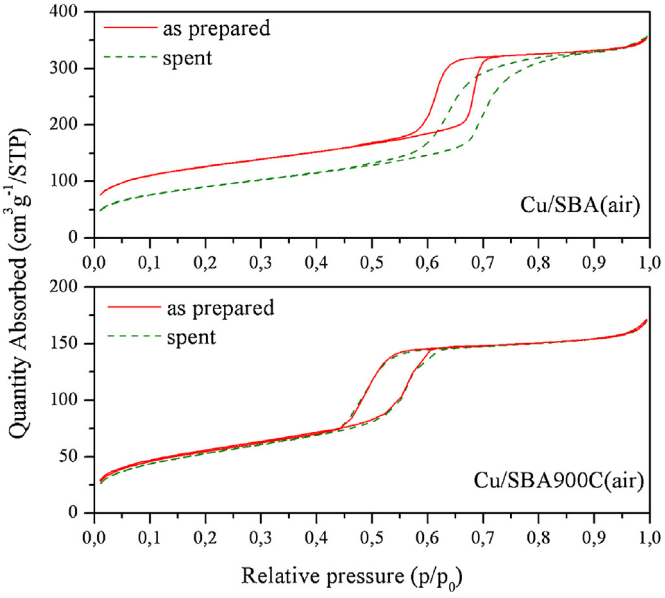

Fig. 13. N_2-physisorption curves of Cu/SBA(air) as-prepared and Cu/SBA900C(air) 3rd time used.

in Fig. 13 for the air calcined samples. For the SBA supported catalyst, the pore structure was affected by the reaction conditions. The adsorption shifted to higher relative pressures and became more gradual, indicating partial loss of the ordered pore structure. The additional heat treatment of SBA900C improved the structural stability of the support under the applied reaction conditions. As can be seen in Fig. 13, the shape of the hysteresis as well as the total pore volume of Cu/SBA900C(air) remained unchanged after performing the reaction. This shows that the increased condensation degree of the silica matrix is beneficial for the application of ordered mesoporous silica supports in liquid, high pressure systems.

4. Conclusions

Highly dispersed copper catalysts on silica gel, SBA and SBA calcined at 900 °C were prepared by a simple impregnation and drying preparation method. The application of various calcination conditions, stagnant air vs air flow and NO flow, greatly influenced the dispersion of copper species. These catalysts showed high activity and selectivity for the selective hydrogenolysis of glycerol. Conversions as high as 50% are obtained at 240 °C, 8 MPa H_2 and 5 h reaction time. Metallic Cu selectively converts glycerol to propylene glycol (selectivity 92–97%) via consecutive dehydration-hydrogenation reactions. The absence of any activity in C—C bond cleavage limits the formation of ethylene glycol and gaseous degradation products. Surface metallic copper (copper surface area) mainly contributes to the performance (mass specific rate). In addition, the activity values of these catalysts (expressed as TOF), renders these materials as extremely active in glycerol hydrogenolysis. The varying initial intrinsic activity correlates with metallic Cu particle size indicating structure sensitivity of the reaction. Importantly, it was observed that the solvent altered the nature of structure sensitivity inducing changes probably related with the rate determining step of the reaction mechanism. The reusability study showed that the air-calcined catalysts were more deactivation resistant, while the NO/N_2 samples suffered from strong deactivation. Sintering of active copper particles resulting in loss of active area was assigned as the major factor contributing to the deactivation profile. In addition, strongly adsorbed species and carbonaceous species on the surface result in loss of active sites and consequently in the observed activity decrease. The structural stability of the SBA-15 support was improved by an additional heat treatment at 900 °C. As a result the Cu/SBA900C(air) catalyst proved to be a stable catalyst, showing no deactivation after three reaction cycles. Finally, the stable performance of the two promising catalysts (Cu/SBA900C(air) and Cu/SG(air)) is attributed to the stability of the supports (silica gel and SBA900) and to the copper morphology obtained under air flow calcination treatment.

Acknowledgements

Efterpi Vasiliadou and Angeliki Lemonidou acknowledge the financial support from European Union-European Regional Development Fund and Ministry of Education, Lifelong Learning and Religious Affairs, ESPA 2007–2013/EPAN II programme, Action 'Synergasia' (project code 1165). Mr George Gkanas, is gratefully acknowledged for his help in the hydrogenolysis experiments. T. M. Eggenhuisen, P. Munnik, and K. P. de Jong acknowledge the Netherlands Organization for Scientific Research for funding (NWO TOP/ECHO 700.57.341).

References

[1] L.C. Meher, R. Gopinath, S.N. Naik, A.K. Dalai, Industrial and Engineering Chemistry Research 48 (2009) 1840–1846.
[2] M. Pagliaro, R. Ciriminna, H. Kimura, M. Rossi, C.D. Pina, Angewandte Chemie International Edition 46 (2007) 4434–4440.
[3] Z. Huang, F. Cui, H. Kang, J. Chen, X. Zhang, C. Xia, Chemistry of Materials 20 (15) (2008) 5090–5099.
[4] Z. Xiao, Zh. Ma, X. Wang, Ch.T. Williams, Ch. Liang, Industrial and Engineering Chemistry Research 50 (4) (2011) 2031–2039.
[5] J. Zheng, W.C. Zhu, C.X. Ma, M.J. Jia, Z.L. Wang, Y.H. Hou, W.X. Zhang, Polish Journal of Chemistry 83 (2009) 1379–1387.
[6] A. Bienholz, F. Schwab, P. Claus, Green Chemistry 12 (2) (2010) 290–295.
[7] C. Liang, Z. Ma, L. Ding, J. Quin, Catalysis Letters 130 (2009) 169–176.
[8] M.A. Dasari, P.P. Kiatsimkul, W.R. Sutterlin, G.J. Suppes, Applied Catalysis A-General 281 (1–2) (2005) 225–231.
[9] E. D'Hondt, S.V.d. Vyver, B.F. Sels, P.A. Jacobs, Chemical Communications 45 (2008) 6011–6012.
[10] D. Roy, B. Subramaniam, R.V. Chaudhari, Catalysis Today 156 (2010) 31–37.
[11] A. Wrawrzetz, B. Peng, A. Hrabar, A. Jentys, A.A. Lemonidou, J.A. Lercher, Journal of Catalysis 269 (2) (2010) 411–420.
[12] Y. Xi, J.E. Holladay, J.G. Frye, A.A. Oberg, J.E. Jackson, D.J. Miller, Organic Process Research & Development 14 (6) (2010) 1304–1312.
[13] A. Torres, D. Roy, B. Subramaniam, R.V. Chaudhari, Industrial & Engineering Chemistry Research 49 (21) (2010) 10826–10835.
[14] Y. Kusunoki, T. Miyazawa, K. Kunimori, K. Tomishige, Catalysis Communications 6 (2005) 645–649.
[15] A. Alhanash, E. Kozhevnikova, V. Kozhevnikov, Catalysis Letters 120 (2008) 307–311.

[16] T. Miyazawa, S. Koso, K. Kunimori, K. Tomishige, Applied Catalysis A-General 318 (2007) 244–251.
[17] D.G. Lahr, B.H. Shanks, Journal of Catalysis 232 (2) (2005) 386–394.
[18] T. Miyazawa, S. Koso, K. Kunimori, K. Tomishige, Applied Catalysis A-General 329 (2007) 30–35.
[19] S. Wang, H. Liu, Catalysis Letters 117 (1) (2007) 62–67.
[20] M. Balaraju, V. Rekha, P.S.S. Prasad, R.B.N. Prasad, N. Lingaiah, Catalysis Letters 126 (2008) 119–124.
[21] J. Zheng, Zh. Wanchun, Ch. Ma, Y. Hou, W. Zhang, Zh. Wang, Reaction Kinetics, Mechanisms, and Catalysis 99 (2010) 455–462.
[22] J. Zhou, L. Guo, X. Guo, J. Mao, Sh. Zhang, Green Chemistry 12 (2010) 1835–1843.
[23] A. Bienholz, H. Hofmann, P. Claus, Applied Catalysis A-General 391 (2011) 153–157.
[24] W. Yu, J. Xu, H. Ma, C. Chen, J. Zhao, H. Miao, Q. Song, Catalysis Communications 11 (2010) 493–497.
[25] W. Yu, J. Zhao, H. Ma, H. Miao, Q. Song, J. Xu, Applied Catalysis A 383 (2010) 73–78.
[26] X. Guo, Y. Li, R. Shi, Q. Liu, E. Zhou, W. Shen, Applied Catalysis A-General 371 (2009) 108–113.
[27] X. Guo, Y. Li, W. Song, W. Shen, Catalysis Letters 141 (2011) 1458–1463.
[28] E.S. Vasiliadou, E. Heracleous, I.A. Vasalos, A.A. Lemonidou, Applied Catalysis B-Environmental 92 (1–2) (2009) 90–99.
[29] E.S. Vasiliadou, A.A. Lemonidou, Organic Process Research & Development 15 (2011) 925–931.
[30] C. Montassier, J. Dumas, P. Granger, J. Barbier, Applied Catalysis A 121 (1995) 231–244.
[31] L.Y. Guo, J.X. Zhou, J.B. Mao, X.W. Guo, G. Zhang, Applied Catalysis A-General 367 (2009) 93–98.
[32] A. Bienholz, R. Blume, A. Knop-Gericke, F. Girgsdies, M. Behrens, P. Claus, Journal of Physical Chemistry C 115 (2011) 999–1005.
[33] E.S. Vasiliadou, A.A. Lemonidou, Applied Catalysis A-General 396 (1–2) (2011) 177–185.
[34] J.R.A. Sietsma, J.D. Meeldijk, J.P. den Breejen, M. Versluijs-Helder, A.J. van Dillen, P.E. de Jongh, K.P. de Jong, Angewandte Chemie International Edition 46 (2007) 4547–4549.
[35] M. Wolters, P. Munnik, J.H. Bitter, P.E. De Jongh, K.P. De Jong, Journal of Physical Chemistry C 115 (8) (2011) 3332–3339.
[36] P. Munnik, M. Wolters, A. Gabrielsson, S.D. Pollington, G. Headdock, J.H. Bitter, P.E. de Jongh, K.P. de Jong, Journal of Physical Chemistry C 115 (2011) 14698–14706.
[37] T. Tsoncheva, Vl Dal Sauto, A. Gallo, N. Scotti, M. Dimitrov, D. Kovacheva, Applied Catalysis A-General 406 (2011) 13–21.
[38] D.Y. Zhao, J.L. Feng, Q.S. Huo, N. Melosh, G.H. Fredrickson, B.F. Chmelka, G.D. Stucky, Science 279 (1998) 548–552.
[39] S. Ek, A. Root, M. Peussa, L. Niinisto, Thermochimica Acta 379 (2001) 201–212.
[40] B.P.C. Hereijgers, R.F. Parton, B.M. Weckhuysen, ACS Catalysis 1 (2011) 1183–1192.
[41] G. Ertl, H. Knozinger, J. Weitkamp, Handbook of Heterogeneous Catalysis, vol. 2, Wiley-VCH, Weinheim, Germany, 1997, pp. 440–441.
[42] E.D. Guerreiro, O.F. Gorriz, J.B. Arrfia, Applied Catalysis A 165 (1997) 259–271.
[43] J.R. Matos, L.P. Mercuri, M. kruk, M. Jaroniec, Chemistry of Materials 13 (2001) 1726–1731.
[44] R.B. Mane, A.M. Hengne, A.A. Ghalwadkar, S. Vijayanand, P.H. Mohite, H.S. Potdar, ChV. Rode, Catalysis Letters 135 (2010) 141–147.
[45] A. Szizybalski, F. Girgsdies, A. Rabis, Y. Wang, M. Niederberger, T. Ressler, Journal of Catalysis 233 (2005) 297–307.
[46] G.C. Chinchen, K.C. Waugh, D.A. Whan, Applied Catalysis 25 (1986) 101–107.
[47] R.S. Rao, A.B. Walters, M.A. Vannice, Journal of Physical Chemistry B 109 (2005) 2086–2092.
[48] X. Zhang, B. Han, y. Li, B. Zhong, Sh. Peng, Journal of Supercritical Fluids 23 (2002) 169–177.
[49] E.A. Gelder, S.D. Jackson, C.M. Lok, Catalysis Letters 84 (2002) 205–208.
[50] Y. Nitta, T. Kubota, Y. Okamoto, Journal of Molecular Catalysis A-Chemical 212 (2004) 155–159.